A High-Selectivity Bandpass Filter Using Dual-Mode Coupling Resonator

José Garibaldi Duarte Júnior[1], João Guilherme Domingos Oliveira[1],
Valdemir Praxedes da Silva Neto[2], Adaildo Gomes D'Assunção[2]
[1]*Programa de Pós-Graduação em Engenharia Elétrica e Computação, Federal University of Rio Grande do Norte, Natal, RN, Brazil, garibaldijrrn@gmail.com, guilhermedomingos@ufrn.edu.br*
[2]*Departamento de Engenharia de Comunicações, Federal University of Rio Grande do Norte Natal, RN, Brazil, valdemir.praxedes@ufrn.br and adaildo@ymail.com*

***Abstract*— In this work, a new model of high selectivity dual-mode bandpass filter is presented. The proposed filter consists of a set of coupled lines with a dual-mode adjustable response in its design process. An improvement in selectivity is presented by combining the dual-mode element with a classic band rejection structure, thus making it possible to introduce transmission zeros near the transmission band. A modeling is presented based on the traditional analysis of even and odd excitation circuit. Circuit and microstrip line simulations are carried out via ADS and Ansoft HFSS, and their results are compared with measurements made on a fabricated prototype. Its results were consistent with those of the process of analysis and synthesis of the high selectivity filter.**

***Index Terms*—** *Bandpass filter, High-selectivity, Coupling lines, Even-Odd modes, Allstop.*

I. INTRODUCTION

Modern telecommunications systems usually have several integrated circuits associated with each other, with filters being a fundamental element in these systems. The development of this type of component has called the attention of several researchers, among the many types of filters implemented, some characteristics are commonly sought given the existing demands in the current scenario of transmission systems, being the low profile, reduced dimensions, low loss by insertion in the crossing bands and high attenuation in the rejection bands, and frequency selectivity. Planar filters have gained increasing prominence among researchers, thus boosting the number of works related to this type of device.

A wide variety of filters in the most diverse topologies have been developed [1]-[15]. In this type of component, the implemented projects can be carried out through n-mode filters, for example, dual-mode single-band and single-wideband [1]-[4], dual-mode and dual-band filters [5]-[6], triple-mode and single-band [7], or even dual-band and quad-mode microwave filters [8]-[11], where each design seeks to achieve specific results, such as the case where asymmetric inductive disturbances are implemented to obtain zero transmission frequencies [1], representing a stub with a short-circuit response, thus obtaining inductive characteristics it is adjusted to control the bandwidth by dividing

  ISSN 2179-1074

two degenerate modes [2].

In certain applications, as in the case of systems where the frequency spectrum is a crucial factor and this needs to be shared by several communication standards, there is a need for communication systems that operate in sufficiently narrow frequency bands so as not to interfere with other nearby frequency bands. Faced with this scenario, researchers have been looking to study and develop devices, such as planar radio frequency filters, with such characteristics. In [12], a high selectivity filter based on quarter-wave lines with four operating bands is proposed, which are dependent on each other, which makes it difficult to synthesize for specific operating ranges. A broadband filter with high selectivity characteristics is developed by [13], and its structure is based on lines coupled with short-circuit stubs, thus obtaining a large dimension structure. In [14], [15] and [21] planar filters based on line stubs with transmission zeros close to the central frequency are developed, thus increasing the frequency response selectivity.

This work proposes a bandpass filter based on pairs of coupled lines with dual-mode response, from the adjustment of electrical lengths and line impedances, a response with high selectivity in the operating band is obtained. A modeling is presented and its analysis is done in terms of the coupling operation modes. Full-wave EM simulations are performed in order to establish a comparative analysis. The location of the transmission zeros is studied in order to obtain the optimized geometry. A prototype is fabricated and measured for comparison purpose. Agreement is observed between simulation (propagating mode analysis and ADS equivalent circuit) and measurement results.

II. High-Selectivity Bandpass Filter Design

A. Dual-mode Resonator Modeling

Dual-mode resonators are characterized by the possibility of adjustment in each of the resonant modes, thus providing degrees of freedom of analysis and synthesis for the various resonant circuits individually. The resonator transmission line circuit modeled in this work is shown in Fig. 1(a), part of its analysis was developed in [16]. Due to the symmetry and presence of the couplings, the resonator is modeled in terms of the circuit resulting from the analysis of even excitation, Fig. 1(b), and the circuit from the analysis of odd excitation, Fig. 1(c).

The resonator structure is composed by the junction of a pair of lines coupled with characteristic admittances Y_{oe}, Y_{oo} and electrical length θ_2, shorted by an admittance open stub load Y_3 and length θ_3. Admittance capacitors Y_c present in the resonator structure terminals model the losses present in the coupled lines, their modeling follows the methodology applied in [16], [17].

Equations (1) and (2) represent the expressions for admittance of a lossless line with characteristic admintance Y_0 and electrical length θ terminated in open circuit and short circuit, respectively.

$$Y_{in,ca} = jY_0 \tan\theta \tag{1}$$

$$Y_{in,cc} = -jY_0 \cot\theta \tag{2}$$

Based on these equations and considering the equal electrical lengths $\theta_1 = \theta_2 = \theta_3 = \theta$ to simplify

  ISSN 2179-1074

the analysis, the expressions for the input admittances to the excitation circuit in Fig. 1(b).

$$Y_{in,a} = j\frac{Y_3}{2}\tan\theta \tag{3}$$

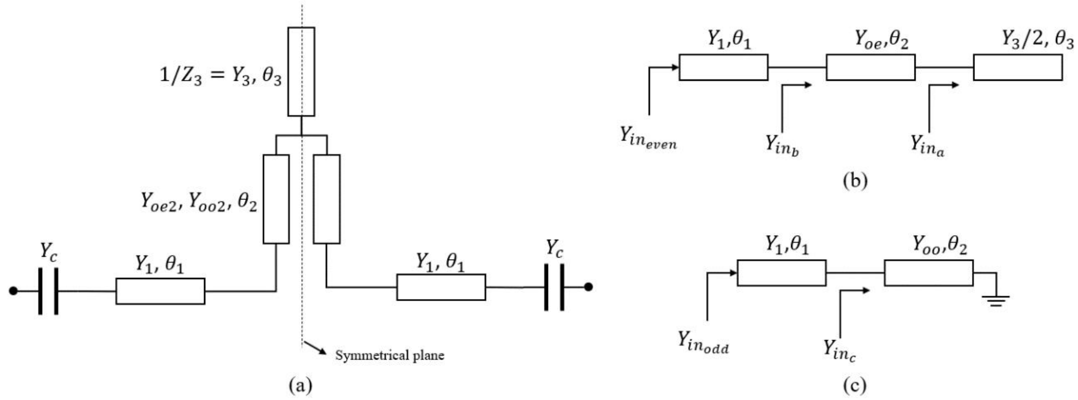

Fig. 1. Dual-mode resonator. (a) Dual-mode resonator structure modeled on a transmission line. (b) Even excitation circuit. (c) Odd excitation circuit.

$$Y_{in,b} = \frac{jY_{oe}\tan\theta\left(Y_3 + 2Y_{oe}\right)}{2Y_{oe} - Y_3\tan^2\theta} \tag{4}$$

$$Y_{in,even} = \frac{jY_1\left[\tan\theta\left(2Y_{oe}^2 + 2Y_{oe}Y_1 + Y_{oe}Y_3\right) - \tan^3\theta\left(Y_1Y_3\right)\right]}{2Y_{oe}Y_1 - \tan^2\theta\left(2Y_{oe}^2 + Y_1Y_3 + Y_{oe}Y_3\right)} \tag{5}$$

Applying the resonance condition, where $Y_{(in,even)}$ equals zero according to equation (6), it is possible to obtain the expression for the resonance frequency given in equation (7), where c is the speed of light in vacuum, L the physical length of the line and ε_{eff} is its effective permittivity [17].

$$\tan\theta\left(2Y_{oe}^2 + 2Y_{oe}Y_1 + Y_{oe}Y_3\right) = \tan^3\theta\left(Y_1Y_3\right) \tag{6}$$

$$f_{even} = \frac{c\tan^{-1}\left(\sqrt{K1}\right)}{2\pi L\sqrt{\varepsilon_{eff}}} \tag{7}$$

$$K1 = \frac{2Y_{oe}^2 + 2Y_{oe}Y_1 + Y_{oe}Y_3}{Y_1Y_3} \tag{8}$$

From the circuit present in Fig. 1 (c), and from equation (2) that models a short-ended line, the input admittance expressions for the even excitation circuit are made. Also applying the resonance condition, there is the expression for the resonance frequency in an odd mode (11).

$$Y_{in,c} = -jY_{oo}\cot\theta \tag{9}$$

$$Y_{in,odd} = \frac{jY_1\left(Y_1\tan^2\theta - Y_{oo}\right)}{\left(Y_1 + Y_{oo}\right)\tan\theta} \tag{10}$$

$$f_{odd} = \frac{c\tan^{-1}\left(\sqrt{K2}\right)}{2\pi L\sqrt{\varepsilon_{eff}}} \tag{11}$$

$$K2 = \frac{Y_{oo}}{Y_1} \tag{12}$$

  ISSN 2179-1074

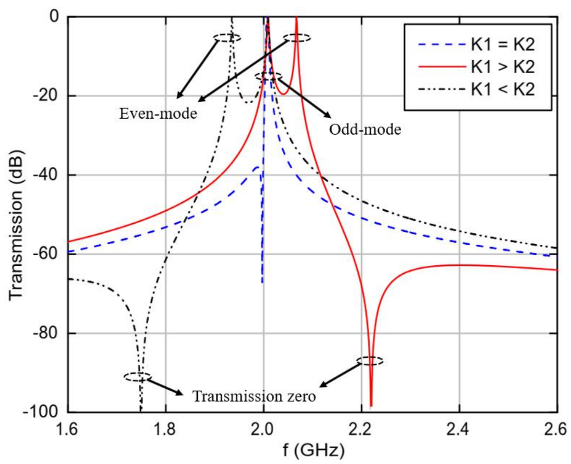

Fig. 2. Transmission coefficient simulated results for the proposed resonator. Effect of the ratio between K1 (even mode) and K2 (odd mode) parameters on the resonator frequency response.

Fig. 2 shows simulated results for the frequency response of the proposed resonator transmission coefficient. For comparison purpose, results are presented for the even and odd mode analyses and for three particular cases: K1=K2, K1>K2 and K1<K2. The calculation of parameters K1 and K2 was carried out using equations (7) - (8) and (10) - (11), for the even and odd mode circuits, respectively, according to the study presented in [17]. For the case where *K1>K2*, the zero-transmission frequency (f_{tz}) appears after the fundamental frequency of the resonator. Similarly, for the situation where *K1<K2*, the f_{tz} occurs before the fundamental resonance frequency. It is important to note that, despite the change in values for *K1* and *K2*, the odd resonance frequency does not change, this can be deduced from the expressions of *K1* and *K2*, where the dependence on Y_3 occurs in only one of these. Therefore, keeping the other admissions constant and varying Y_3, only the even resonance frequency will be changed. The scenario of a single resonance occurs exclusively when *K1* is equal to *K2*, that is, the expressions (7) and (11) are equal. Equation (13) brings the expression of Y_3 for the case of single resonance ($f_{even} = f_{odd}$).

$$Y_3 = \frac{2Y_{oe}^2 + 2Y_{oe}Y_1}{Y_{oo} - Y_{oe}} \tag{13}$$

Fig. 3 shows the frequency responses of S11 and S21 for five different values of Z3 impedance, namely 24.7 Ω, 29.7 Ω, 34.7 Ω, 39.7 Ω and 45.7 Ω. Moreover, the variation of the Z3 impedance value, and hence of the admittance value of the open stub-load, has provided different resonance frequency values. For example, for Z3 equal to 24.7 Ω, a single resonance frequency is observed at 2.2 GHz, for the even mode. However, for Z3 equal to 45.7 Ω, two resonance frequencies are observed at 2.18 GHz and 2.45 GHz. This effect of the variation of Z3 is due to the offset on the frequency of the resonant modes. It is important to emphasize that despite the variation of Z3, for the even mode, the observed odd mode resonance frequencies are about the same at 2.2 GHz. Regarding the transmission coefficient curves in Fig. 3(b), for K1 > K2, the increase in Z3 causes a departure of the resonant mode frequencies as well as of zero-transmission frequency (ftz) with respect to the transmission coefficient bands.

Considering input admittances Y_0 on both ports of the proposed resonator (Fig. 1 (a)), it is possible from the analysis made in [18] to obtain the scattering parameter S21 of the circuit as a quadripole.

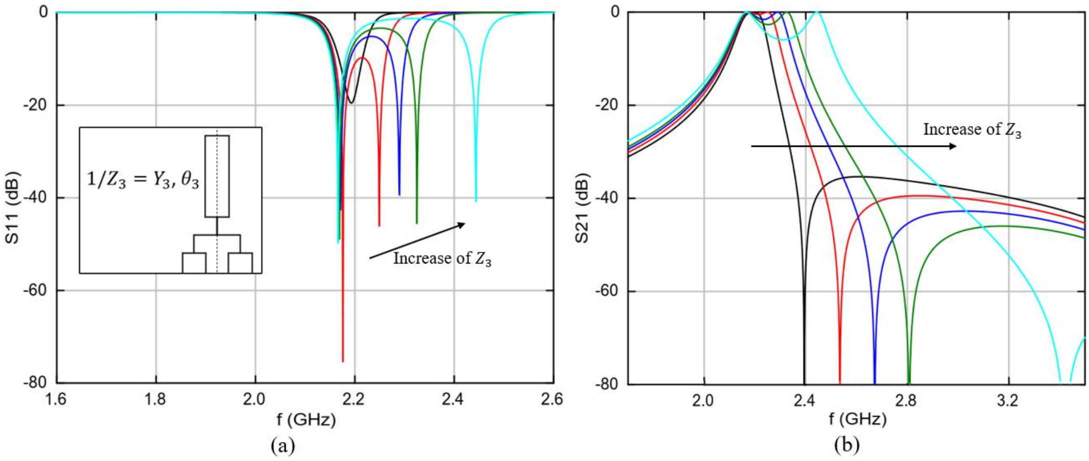

Fig. 3. Resonator frequency response for various values of Z_3. (a) S_{11}. (b) S_{21}.

$$S_{21} = \frac{Y_0\left(Y_{in,odd} - Y_{in,even}\right)}{Y_0^2 + Y_0\left(Y_{in,odd} + Y_{in,even}\right) + Y_{in,odd}Y_{in,even}} \tag{14}$$

By making S21 equal to zero, it is possible to arrive at an expression for the resonator's zero transmission frequency. Soon,

$$S_{21} = 0 \rightarrow Y_{in,odd} = Y_{in,even} \tag{15}$$

Considering equations (5) and (10), we obtain f_{tz}:

$$f_{tz} = \frac{c\tan^{-1}\left(\sqrt{\delta}\right)}{2\pi L\sqrt{\varepsilon_{eff}}} \tag{16}$$

$$\delta = \frac{-a_2 - \sqrt{a_2^2 - 4a_1a_3}}{2a_1} \tag{17}$$

$$a_1 = 2Y_{oe}^2 + Y_3Y_{oe} - Y_3Y_{oo} \tag{18}$$

$$a_2 = 2Y_{oe}^2 + Y_3Y_{oe} - Y_3Y_{oo} + 2Y_{oe}Y_{oo} \tag{19}$$

$$a_3 = a_2 - a_1 \tag{20}$$

By replacing the capacitors together with the impedance lines Y_3 by pairs of coupled lines (Y_{oe1}, Y_{oo1}, θ_1) of equal frequency response following the filter topology based on coupled lines of [18], the circuit simulation was performed resulting from the modeling of the bandpass filter in the ADS (Advanced Design System) software. The frequency response optimized for 2 GHz is shown in Fig. 4. The two modes near the central frequency and the f_{tz} are observed, following the case of $K1 > K2$.

B. Addition of Transmission Zero

According to the analysis of the dual-mode bandpass filter presented so far, its frequency response has only one transmission zero point close to its operating band. In this topic, an addition to the filter geometry will be proposed in order to generate a new zero transmission frequency without causing severe changes in the design of the rest of the filter, and in this way, improve the selectivity in the

  ISSN 2179-1074

transmission band.

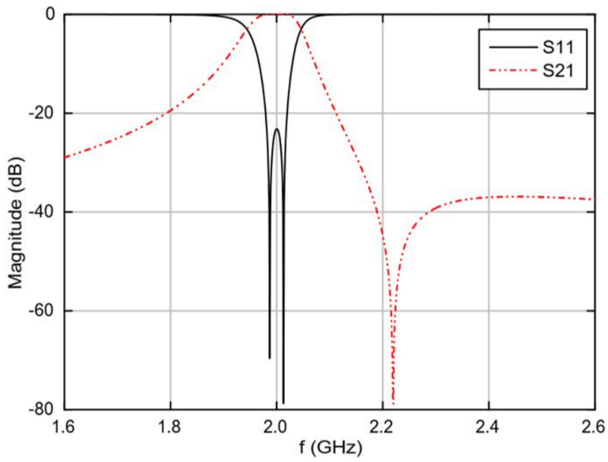

Fig. 4. Simulation of the frequency response of the circuit resulting from the modeling of the bandpass filter.

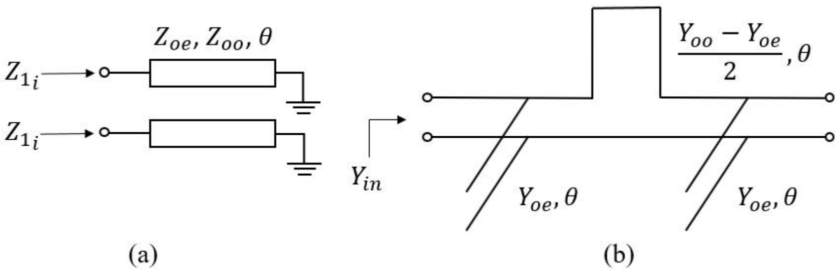

Fig. 5. (a) Topology of the Allstop structure. (b) Diagram of the equivalent circuit related to the input admintance.

Based on the classic topologies formulated in [19], [20], the named allstop structure is formed by a pair of short-circuited coupled lines, as shown in Fig. 5. Its frequency response provides resonance points of zero transmission as a function of electrical length θ of the coupled line pair. The impedances Z_{oe} and Z_{oo} define the level of transmission across the spectrum. Equations (21) - (23) present the formulation of the parameters that govern the modeling of the structure.

$$y_{11} - y_{12} =- jY_{oo} \cot\theta \tag{21}$$

$$y_{12} =- j\frac{(Y_{oo} - Y_{oe})}{2}\cot\theta \tag{22}$$

$$\frac{1}{Y_{in_i}} = Z_{in_i} = j\sqrt{Z_{oo}Z_{oe}}\tan\theta \tag{23}$$

In order to provide a second zero transmission in the frequency response of the dual-mode filter, the allstop structure was coupled to the filter in parallel. Table 1 shows the summary of the impedances adopted for the operation of the bandpass filter with selectivity improvement at 2 GHz. Fig. 6 presents the configuration of the new dual-mode filter geometry with its improved selectivity and its respective frequency response obtained via simulation of the transmission line circuit in the ADS compared to the previous model. It is possible to observe the increase in selectivity on both sides of the filter transmission band, as well as the zero-transmission frequency added. Note also, the two 50 Ω lines

  ISSN 2179-1074

added to the filter ports to facilitate its manufacturing process.

TABLE I. IMPEDANCE SUMMARY OF THE TRANSMISSION LINE CIRCUIT MODEL OF THE BANDPASS FILTER.

Element	Impedance (Ω)	Element	Impedance (Ω)
Z_{oe1}	100	Z_3	53
Z_{oo1}	63	$Z_{oeallstop}$	100
Z_{oe2}	100	$Z_{ooallstop}$	83
Z_{oo2}	50		

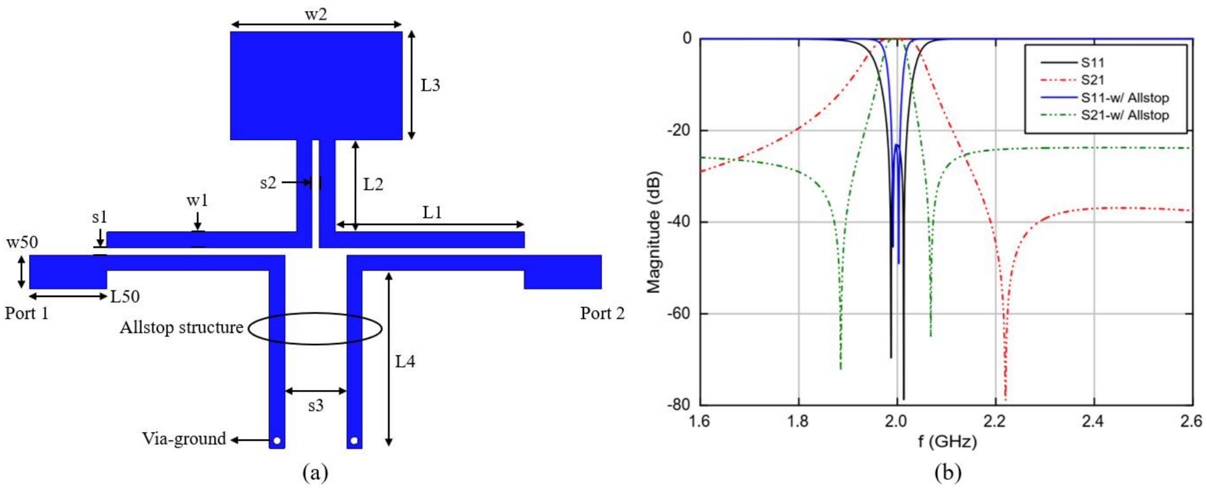

Fig. 6. (a) Bandpass filter with its respective dimensions in mm: w50 = 2.15, L50 = 5.00, s1 = 0.52, w1 = 1.00, s2 = 0.50, w2 = 11.12, L2 = 5.97, L3 = 7.00, L1 = 12.26, s3 = 4.00, L4 = 11.50, track diameter = 0.50. (b) Comparison of the simulated frequency response via the transmission line circuit between the model without and with the allstop structure.

III. RESULTS AND DISCUSSIONS

In view of the presented modeling, a model was developed in the Ansoft HFSS software and a prototype was built in microstrip technology from a RO3006 substrate with a permittivity of 6.35, a tangent of losses of 0.0024 and a height of 1.52 mm, following the physical dimensions present in Fig. 6 (a). Full-wave simulations and experimental measurements were carried out in a network analyzer in order to obtain the scattering parameters S11 and S21 of the filter frequency response. Fig. 7 shows the simulation via HFSS of the current surface density distribution considering the three frequencies under study: transmission frequency (2.00 GHz) and both zero transmission frequencies (1.81 and 2.20 GHz). It is observed that at the transmission frequency a higher surface current density is identified in the central region of the coupled line (Yoe_2, Yoo_2, θ_2). While in other frequencies the distribution is less accentuated in this region. The comparison between the results obtained via simulation and measurement are shown in Fig. 8 (a). The resonance frequency obtained both in the simulation level and in the measurement was 2 GHz with a percentage bandwidth in -3 dB of 3.5% from the measurement. The bandpass filter showed an insertion loss (IL) of 1.34 dB at the main frequency with a return loss greater than 20 dB. A summary of the results obtained is summarized in Table 2 as well as parameters of other studies found in the literature regarding high selectivity

ISSN 2179-1074

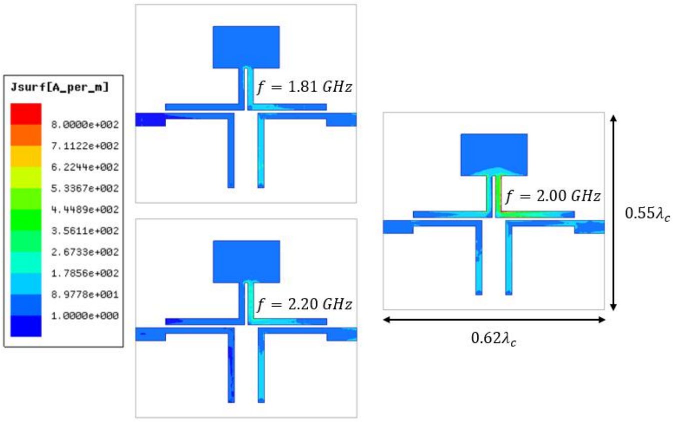

Fig. 7. Simulation of current surface density distribution for the three key frequencies: transmit frequency and the two zero transmit frequencies.

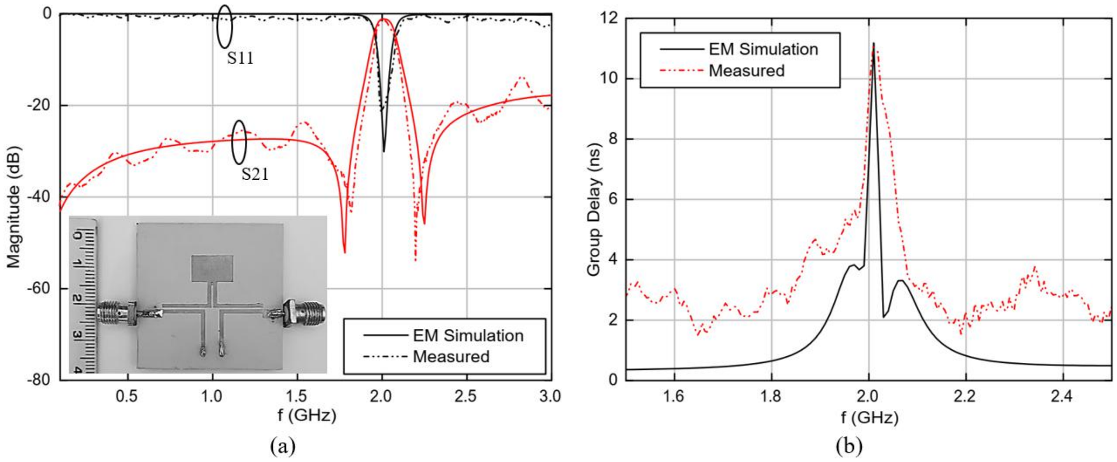

Fig. 8. Frequency response – comparison between result obtained via EM simulation and measurement. (a) Scattering parameters (S11[dB] and S21[dB]). (b) Group Delay[ns].

bandpass filters. The group delay parameter is shown in Fig. 8 (b), with a maximum value of 11 ns for the filter operating band. The zero transmission frequencies obtained were close to 1.81 (lower) and 2.20 GHz (upper), with slopes of 250 and 316 dB/GHz being observed in the lower and upper transition bands, respectively.

TABLE II. COMPARISON BETWEEN HIGH-SELECTIVITY FILTER WORKS.

References	Central Frequency	Fract. Band (%)	Insert. Loss (dB)	Numb. of TZs	Circ. Size (λ_0)
[12]	1.97/4.1/4.6/6.1	13.7/5/5.9/7.6	0.97/1.28/1.78/2.16	8	0.11 x 0.07
[13]	2.05	60	0.60	3	0.48 x 0.24
[14]	2.1	23.7	1.6	4	-
[21]	2	71.5	0.35	5	0.40 x 0.40
This Work	2	3.5	1.34	2	0.55 x 0.62

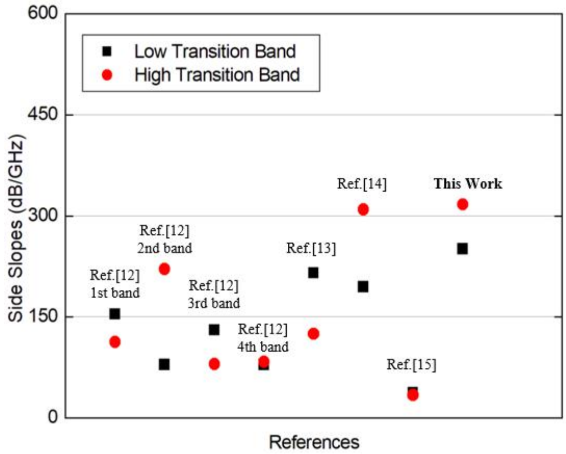

Fig. 9. Comparison of Side Slopes in dB/GHz between works in the literature involving high-selectivity filters and the one developed in this work.

Fig. 9 shows the comparison of the slopes in the transition bands of the selective filters of some references in the literature and in this work. As can be analyzed, the parameters of this work are presented according to the proposal to improve the selectivity of the dual-mode filter in the frequency of 2 GHz.

IV. Conclusion

In this work, a new model of bandpass filter with improvement in its selectivity characteristic is presented. Its configuration is based on the use of a resonator with dual-mode response through the composition of coupled lines short-circuited with a relatively low impedance line terminated in open. The improvement in selectivity comes from the use of the classic allstop element put in parallel with the dual-mode structure. The filter was modeled and analyzed through its respective even and odd excitation circuits. Simulations of the transmission line circuit and full wave analysis in a synthesized model were performed. Its results were compared with experimental measurements made on a prototype built on microstrip technology, which proved its performance as expected. The model then presents itself as a potential device for communication systems with needs for selectivity in the spectrum.

Acknowledgment

This work was supported by CNPq under covenant 573939/2008-0 (INCT-CSF), CAPES and Federal University of Rio Grande do Norte (UFRN).

References

[1] T. W. Lin, J. T. Kuo, S. J. Chung, "Dual-mode ring resonator bandpass filter with asymmetric inductive coupling and its miniaturization," *IEEE Trans. Microw. Theory and Tech.*, vol. 60, pp. 2808-2814, 2012.

[2] S. J. Sun, B. Wu, T. Su, K. Deng, C. H. Liang, "Wideband dual-mode microstrip filter using short-ended resonator with centrally loaded inductive stub," *IEEE Trans. Microw. Theory and Tech.*, vol. 60, pp. 3667-3673, 2012.

[3] W. Feng, X. Gao, W. Che, W., Q. Xue, “Bandpass filter loaded with open stubs using dual-mode ring resonator,” *IEEE Microw. and Wire. Comp. Letters*, vol. 25, pp. 295-297, 2015.

[4] H. Hu, K. L. Wu, “A TM11 Dual-Mode Dielectric Resonator Filter With Planar Coupling Configuration,” *IEEE Trans. Microw. Theory and Tech.*, vol. 61, pp. 131-138, 2012.

[5] H. S. Peng, Y. C. Chiang, “Microstrip diplexer constructed with new types of dual-mode ring filters,” *IEEE Microw. and Wire. Comp. Letters*, vol. 25, pp. 7-9, 2014.

[6] J. K. Ali, H. Alsaedi, M. F. Hasan, H. A. Hammas, “A Peano fractal-based dual-mode microstrip bandpass filters for wireless communication systems,” In *PIERS Proc.* pp. 888-892, 2012.

[7] H. J. Tsai, N. W. Chen, S. K. Jeng, “Center frequency and bandwidth controllable microstrip bandpass filter design using loop-shaped dual-mode resonator,” *IEEE Trans. Microw. Theory Tech.*, vol. 61, pp. 3590-3600, 2013.

[8] A. Ebrahimi, W. Withayachumnankul, S. F. Al-Sarawi, D. Abbott, “Compact dual-mode wideband filter based on complementary split-ring resonator,” *IEEE Microw. and Wire. Comp. Letters*, vol. 24, pp. 152-154, 2013.

[9] M. Alqaisy, C. Chakrabraty, J. Ali, A. R. Alhawari, “A miniature fractal-based dual-mode dual-band microstrip bandpass filter design,” *Intern. Journal of Microw. and Wire. Tech.*, vol. 7, pp. 127-133, 2015.

[10] Y. S. Mezaal, H. T. Eyyuboglu, J. K. Ali, “New dual band dual-mode microstrip patch bandpass filter designs based on Sierpinski fractal geometry,” In *2013 Third International Conference on Advanced Computing and Communication Technologies (ACCT)* , pp. 348-352, 2013.

[11] X. C. Zhu, W. Hong, K. Wu, H. J. Tang, C. Z. Hao, J. X. Chen, P. Chu, “Design and implementation of a triple-mode planar filter,” *IEEE Microw. and Wire. Comp. Letters*, vol. 23, pp. 243-245, 2013.

[12] H. Liu, B. Ren, X. Guan, X., J. Lei, S. Li, “Compact dual-band bandpass filter using quadruple-mode square ring loaded resonator (SRLR),” *IEEE Microw. and Wire. Comp. letters*, vol. 23, pp.181-183, 2013.

[13] K. D. Xu, D. Li, Y. Liu, “High-selectivity wideband bandpass filter using simple coupled lines with multiple transmission poles and zeros,” *IEEE Microw. and Wire. Comp. Letters*, vol. 29, pp. 107-109, 2019.

[14] L. Gao, , X. Y. Zhang, “High-selectivity dual-band bandpass filter using a quad-mode resonator with source-load coupling,” *IEEE Microw. and Wire. Comp. Letters*, vol. 23, pp. 474-476, 2013.

[15] J. G. Duarte, , V. P. D. Silva, “A novel tri-bandpass filter side-coupled square ring based,” *Journal of Microwaves, Optoelectronics and Electromagnetic Applications*, vol. 19, pp. 265-275, 2020.

[16] W-Y. Chen, , M-H Weng, S-J Chang, “A new tri-band bandpass filter based on stub-loaded step-impedance resonator,” *IEEE Microw. and Wire. Comp. Letters*, vol. 22, pp.179-181, 2012.

[17] C. Hua, C.Chen, C. Miao, W. Wu, “Microstrip bandpass filters using dual-mode resonators with internal coupled lines,” *Progress Electro. Res*., vol. 21, pp. 99-111, 2011.

[18] M. Michiaki, H. Yabuki, M. Makimoto, “Dual-mode stepped-impedance ring resonator for bandpass filter applications,” *IEEE Trans.Microw. Theory Tech.,* vol. 49, pp. 1235-1240, 2001.

[19] R. K. Mongia, et al. RF and microwave coupled-line circuits. Artech house, 2007.

[20] D. M. Pozar, Microwave engineering, John Wiley & Sons, 2009.

[21] W. Chen, Y. Wu, , W. Wang, “Planar wideband high-selectivity impedance-transforming differential bandpass filter with deep common-mode suppression,” *IEEE Transactions on Circuits and Systems II: Express Briefs*, vol. 67, pp. 1914-1918, 2019.